Historic, archived document

Do not assume content reflects current scientific knowledge, policies, or practices.

Pacific
North
West Forest and Range Experiment Station
A. Forest Service RESEARCH NOTE

PNW-136 December 1970

PRELIMINARY STUDY OF DYNAMIC CHARACTERISTICS OF SKYLINE LOGGING

by

Ward W. Carson, *Research Mechanical Engineer*

PSW FOREST AND RANGE
EXPERIMENT STATION
JUL 12 1971
STATION LIBRARY COPY

ABSTRACT

Skyline logging systems are used extensively for harvesting timber in rough terrain. Their design and operation depend upon a knowledge of static and dynamic characteristics of the system. This note discusses the results of a preliminary study of the dynamic characteristics of skyline logging.

1.0 INTRODUCTION

Skyline logging systems, used extensively for harvesting timber in rough terrain where a dense road system is undesirable, involve cables or wire ropes suitably anchored and tensioned. A concentrated log load is supported in the span between the anchor points and transported to another point in the span, called a landing. A yarder, located at one anchor point in the cable system, provides the powered drums used to manipulate the cables in the log yarding process.

The logging industry has used skylines for years. Although the design details of these systems were greatly ignored in the past, emphasis on operational efficiency and more sophisticated yarder designs have generated a requirement for more technical knowledge of these cable systems. Broken skylines and anchor failures are becoming common--17 known cases were recorded in the 1969 operating season alone. One such failure resulted in a quarter of a million dollars of timber being burned. Most of these failures are directly attributable to a lack of appreciation for the statics and dynamics of skyline design.

The logging industry needs better design tools with which to treat the layout of skyline systems and the design of the equipment to be used in these systems. Information on the dynamic characteristics of these systems required to implement these tools is not available.

This research note describes the problems related to a study of skyline logging dynamics. Previous work in the field is summarized, and the results of preliminary studies are reported.

1.1 Skyline Configurations

Several configurations of skylines are employed by the logging industry. Those most common, shown in figures 1, 2, and 3, are considered here.

1.1.1 Standing skyline (fig. 1)

This configuration consists of a fixed length of suspended cable (the skyline) anchored at a tailhold (usually a stump) and a headspar (usually a metal tower attached to the yarder). The log load is attached to a carriage, designed to roll freely on the skyline. The carriage and log are drawn along the skyline with another cable, the main line, which is powered by a drum on the yarder.

1.1.2 Live skyline (fig. 2)

This configuration is identical to the standing skyline except that the skyline length can be adjusted at the yarder during the process of picking up and yarding the log. While the skyline is anchored at the tailhold, the length is adjusted at the yarder end by a powered drum. The main line and carriage operate as in the standing skyline configuration.

1.1.3 Running skyline (fig. 3)

This configuration is similar to the live skyline except that the skyline, in this case called a haulback, continues through a block at the tailhold and terminates at the carriage. This feature allows the system to operate on any slope, whereas the standing and live skyline systems depend upon gravity location of the carriage. Again, the main line operates as in the other configurations.

1.2 Loading

The ratio of live load to dead load in a logging skyline clearly distinguishes it from other suspension structures such as bridges and roofs. The nature of the rough terrain where skylines are commonly operated presents several interesting loading situations. The forcing functions defined here represent typical loading situations expected to generate critical cable tensions or operational problems for the yarding equipment.

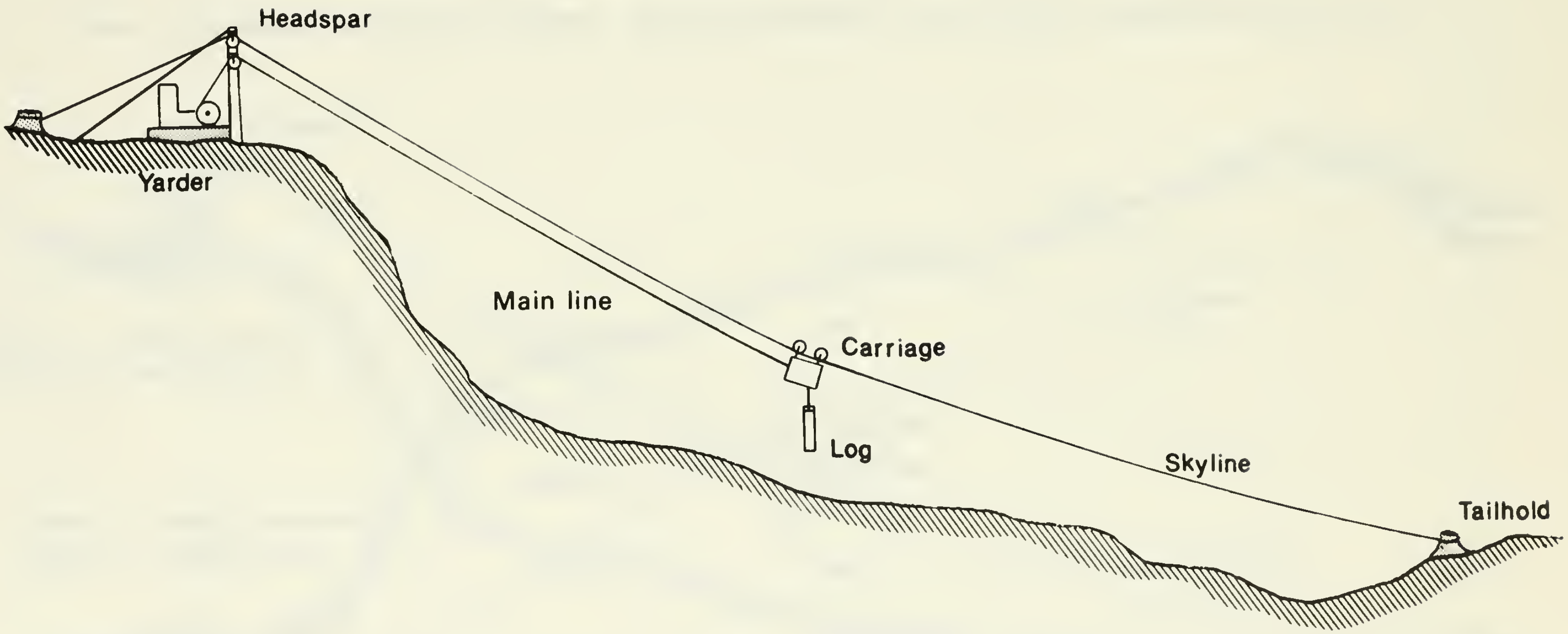

Figure 1.—Standing skyline, gravity carriage.

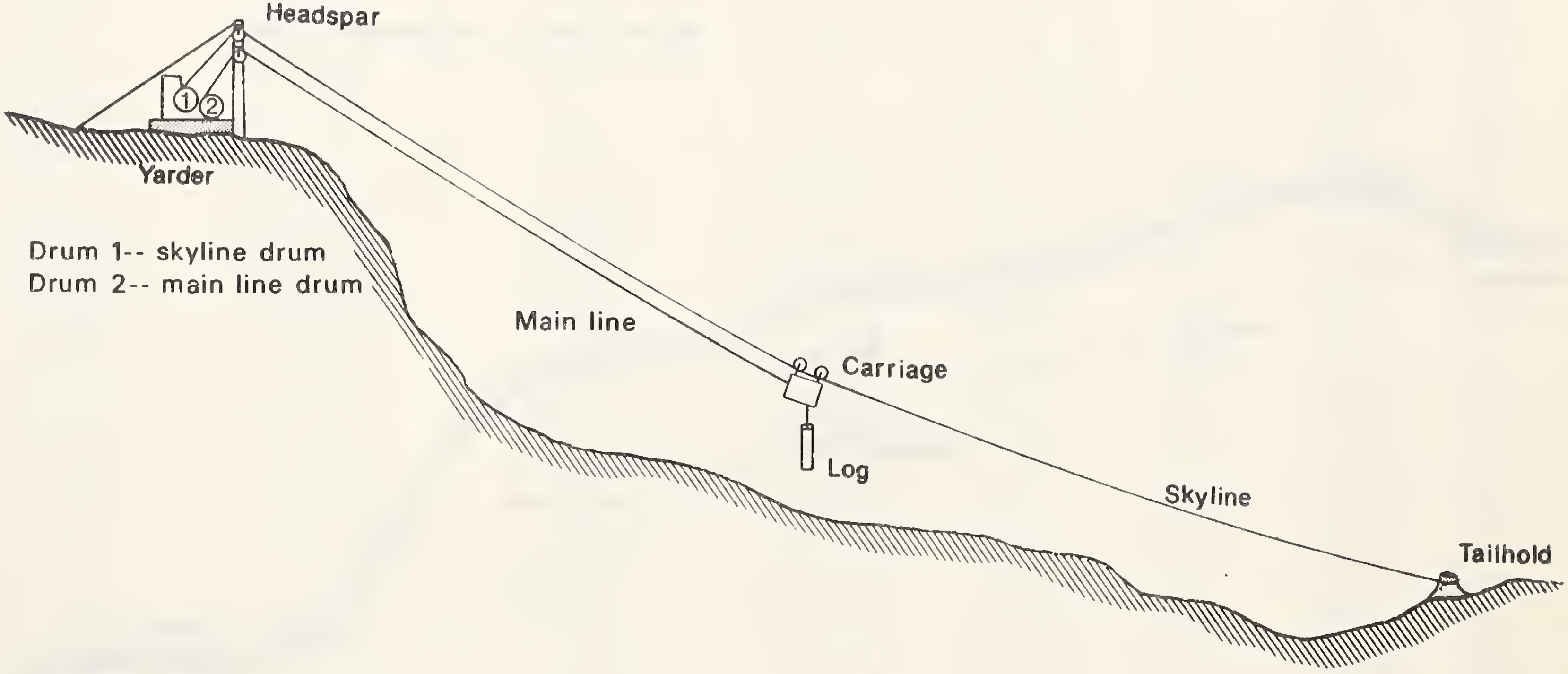

Figure 2.—Live (slackline) skyline, gravity carriage. Skyline drum powered so skyline length is varied during yarding operation.

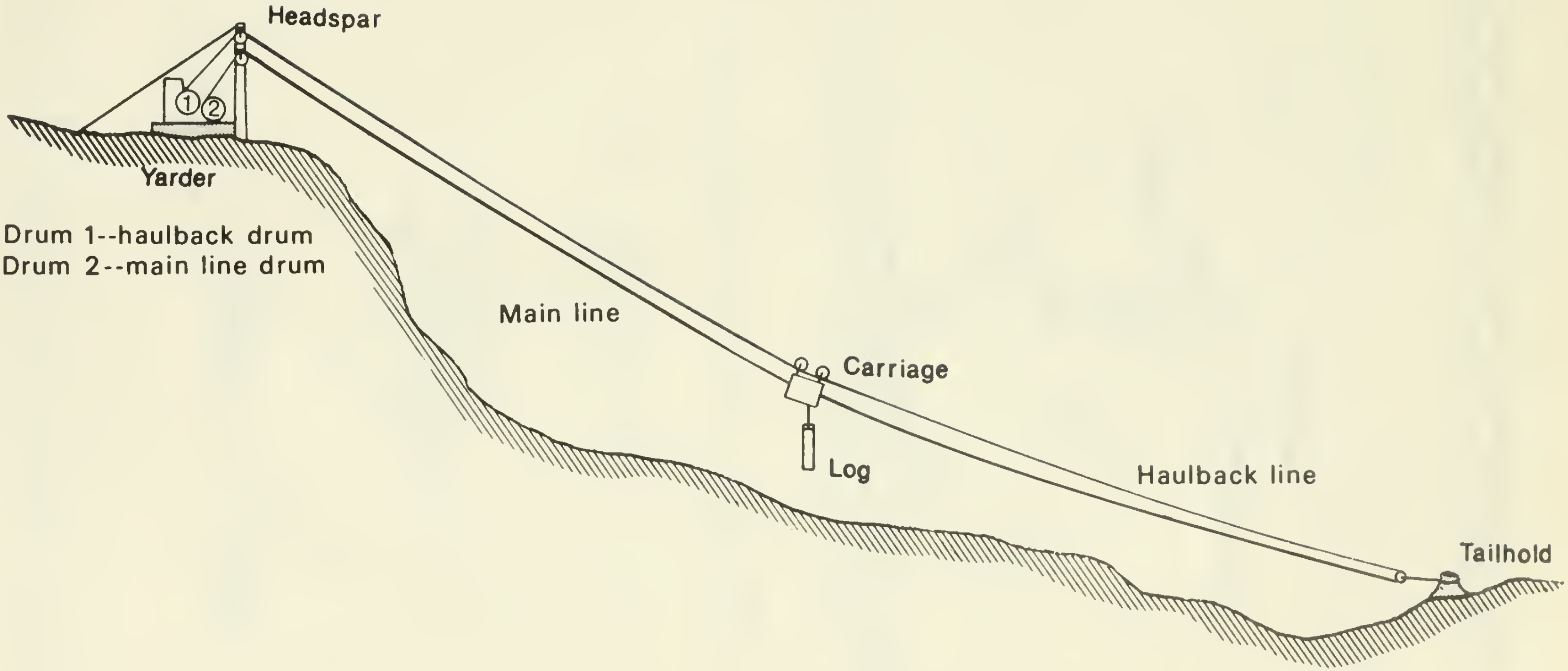

Figure 3.—Running skyline. Drums 1 and 2 on the yarder are interlocked for horsepower exchange during yarding operation.

During yarding, a log load will at times go from being partially supported by the ground to being freely suspended, as when the log falls off a high point in the terrain.

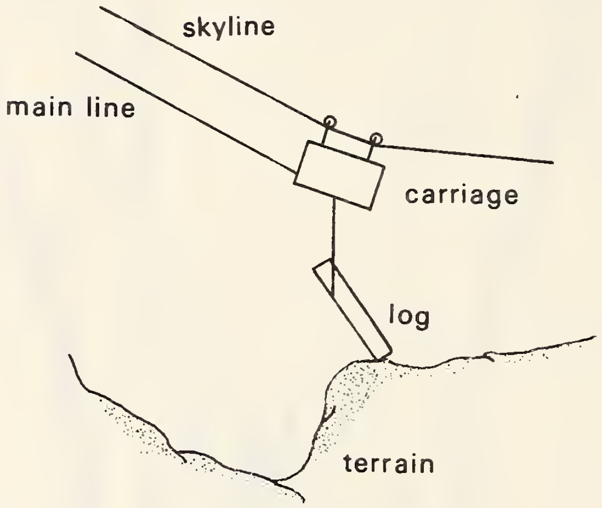

Suddenly applied concentrated mass.

A log being dragged at some velocity will commonly get "hung up" by some obstacle in the terrain.

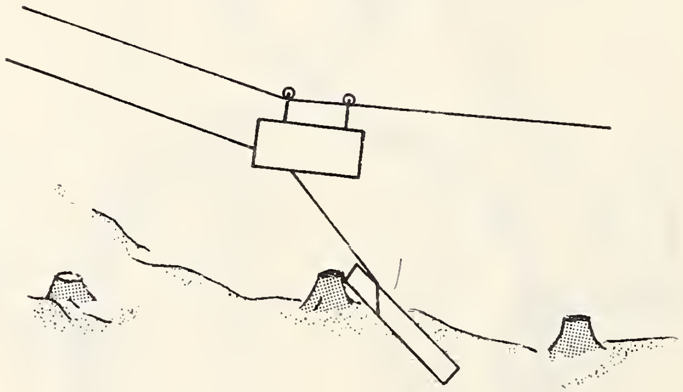

Stoppage of horizontal travel.

Frictional forces developed at the ground during normal yarding cause heavy logs to move in an oscillatory motion.

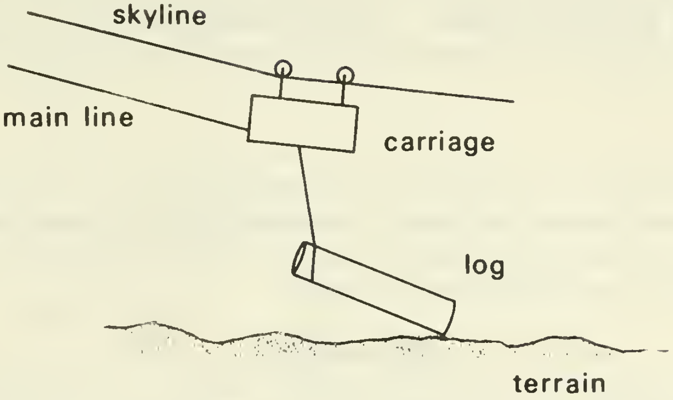

Normal dragging of heavy log.

When the load is "hung up," the yarder operator will usually tension all lines in an attempt to free the load. If the load comes free, the vibration of the cable is not expected to generate dangerous tensions; however, the input to the yarder and its response should prove interesting.

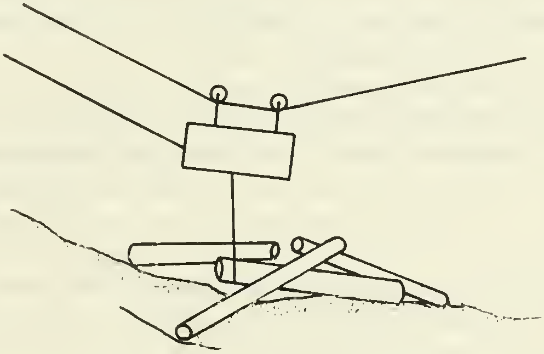

Log "hung up" under other logs.

2.0 BACKGROUND

Before the problem was analyzed, the literature of related work was reviewed and is summarized in this section.

2.1 Static

The mathematical formulation of the static skyline problem is treated under the more general classification of catenary problems *(8)*. Specific treatment of logging skylines supporting concentrated loads appeared in a paper by Anderson *(2)* and in a later work by Mills *(10)*. These papers establish the mathematical formulation of the problem and give closed-form expressions for the skyline variables.

The catenary description of the static skyline problem consists of a set of nonlinear, transcendental equations. The number of equations is directly related to the number of cable segments in the configuration. Although solution of these equations presents a difficult numerical problem, the problem has been treated extensively by several investigators *(5, 12, 13)*.

2.2 Dynamic

The transverse vibration of a heavy, taut string is a classic problem in wave motion. With assumptions of small variations in tension and small deflections, the string's behavior is described by the familiar wave equation,

$$\frac{\partial^2 y}{\partial x^2} = \frac{\rho}{T} \frac{\partial^2 y}{\partial t^2} .$$

Many problems described by this equation have been solved *(7)*.

The first extensive analysis of the nonlinear problem was done by Carrier *(3, 4)*. Carrier applied first the perturbation method *(3)* and later a method using an analogy with the boundary layer problem *(4)*. Both methods were approximations for the range of moderately large amplitude vibrations and were primarily concerned with the propagation of localized deformations.

The oscillatory failure of the Tacoma Narrows bridge *(1)* stimulated considerable interest in cable vibrations in response to aerodynamically generated oscillatory loadings. The primary concern of this analytical work *(15, 16, 17, 21)* was to predict the structure's natural frequencies of vibration. Considerable experimental work was done with models to develop and substantiate semiempirical expressions for natural frequencies as a function of span, deflection, mass, etc. The philosophy was to develop extremely conservative designs in terms of keeping the natural frequencies away from the aerodynamic eddy frequency as predicted by the Von Karman vortex theory.

The response of an elastic, uniform, flexible cable to a suddenly imposed velocity at some point of its length has been examined by a number of investigators *(6, 11, 18)*. These studies were promoted primarily by an interest in design of arresting cables for aircraft on naval aircraft carriers. Ringleb *(18)* presented a particularly interesting analysis of the motion and stress of an initially straight elastic cable subjected to impact. He was able to develop closed-form solutions for stress, transverse and longitudinal motion, and energy in cables subjected to impact loads. Although the limited geometry of Ringleb's problem does not make it directly applicable to the skyline logging problem, it should be of valuable assistance.

Some work has been done on the cable dynamics associated with towing submerged bodies, such as sonar vehicles or oceanographic instrument packages *(20)*. This work was restricted to one-dimensional geometry with the boundary conditions of a large mass on the opposite end of a tether experiencing large amplitude, sinusoidal oscillations.

The most recent work in cable dynamics has been stimulated by an interest in suspended roof structures. Architects have promoted the use of these structures where long spans are required *(9, 14, 24)*. Although the literature for static design is fairly complete *(12, 19)*, the dynamics have received very little treatment. Individual designs have been modeled and tested for response to wind and seismic loading *(22, 23)*, but little has been done in the way of general theory. Mollmann *(12)* has analyzed the single cable for both static and dynamic characteristics; however, small vibrations are assumed in the dynamic treatment.

No work, apparently, has been done on the dynamics of logging cable systems. Some experimental data have been collected by this Station; however, the difficulty and expense of measuring and controlling parameters have prohibited completion of most of these tests.

3.0 PROBLEM FORMULATION

Cables, when treated as a subject in mechanics, are often assumed to be inextensible and completely flexible. Assumptions of small deflections and approximately constant tensions also are conveniently applied to maintain the linearity of the problem. In the present formulation, only the assumption of complete flexibility will be retained. The equations developed are highly nonlinear and a finite difference approach to solution is discussed.

3.1 Problem Geometry

The two-dimensional geometry of three specific states of a cable are of interest in this problem: the unstrained state, the initial state, and the final state.

The unstrained state is the natural condition of the cable when the cable force is zero. The geometry of this state is not of interest; however, it serves as a convenient reference in the stress-strain and strain-displacement expressions, and its relationship to the other states will be important.

The initial state is the static equilibrium configuration of the cable due to a given load. The position vector (fig. 4) describing this state in Cartesian coordinates is taken as:

$$\vec{r}(s) = x(s)\vec{i} + y(s)\vec{j} \ ,$$

where s is the arc length in this state and is taken as a parameter, x,y are Cartesian coordinates of figure 4, and $\vec{i},\vec{j}$ are the unit vectors of the coordinate system.

The final state of the cable is the configuration existing at anytime t. Its position vector is related to the initial state through

$$\vec{R}(s) = \vec{r}(s) + \vec{u}(s) \ ,$$

where $\vec{u}(s)$ is called the displacement vector and has Cartesian components.

$$\vec{u}(s) = v(s)\vec{i} + w(s)\vec{j}$$

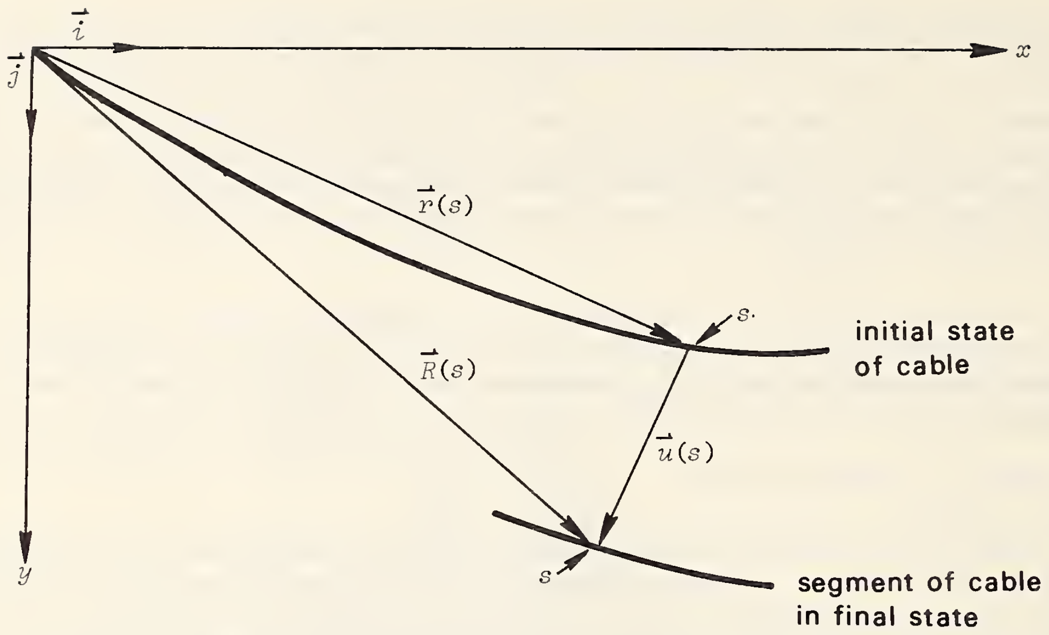

Figure 4.—Problem geometry.

The unit tangent vectors at any point in both the initial and final positions are required. These are expressed as

$$\vec{t}_{\text{initial}} = \frac{\dfrac{\partial x}{\partial s}\vec{i} + \dfrac{\partial y}{\partial s}\vec{j}}{\sqrt{\left(\dfrac{\partial x}{\partial s}\right)^2 + \left(\dfrac{\partial y}{\partial s}\right)^2}}$$

and

$$\vec{t}_{\text{final}} = \frac{\left(\dfrac{\partial x}{\partial s} + \dfrac{\partial v}{\partial s}\right)\vec{i} + \left(\dfrac{\partial y}{\partial s} + \dfrac{\partial w}{\partial s}\right)\vec{j}}{\sqrt{\left(\dfrac{\partial x}{\partial s} + \dfrac{\partial v}{\partial s}\right)^2 + \left(\dfrac{\partial y}{\partial s} + \dfrac{\partial w}{\partial s}\right)^2}} \; .$$

3.2 Stress-Strain Relationship

A linear stress-strain relationship is assumed which is referenced to the arc length of the cable in the unstrained state, namely,

$$T = EA\,\frac{dS - ds_o}{ds_o}$$

or

$$T = EA\,\gamma_o \;\; ,$$

where

T = the tension,
E = Young's modulus for the cable,
A = the reference cross-sectional area of the cable,
dS = the cable element arc length in some final state,
ds_o = the cable element arc length in the unstrained state,

and, as indicated,

$$\gamma_o = \frac{dS - ds_o}{ds_o} .$$

This stress-strain relationship assumes that the cross-sectional dimension of the cable, small compared to its length, changes negligibly with tension.

Tension is the only force considered at a cable cross section. Bending resistance is considered negligible.

3.3 Strain-Displacement Relationship

The element arc lengths for the initial and final states are expressed in terms of the position vectors. We have for the initial state,

$$dr = \left(\left(\frac{\partial x}{\partial s}\right)^2 + \left(\frac{\partial y}{\partial s}\right)^2\right)^{1/2} ds$$

and for the element arc length in the final state,

$$dR = \left(\left(\frac{\partial x}{\partial s} + \frac{\partial v}{\partial s}\right)^2 + \left(\frac{\partial y}{\partial s} + \frac{\partial w}{\partial s}\right)^2\right)^{1/2} ds .$$

The element arc length in the unstrained state must be derived from the initial state and the stress-strain relationship. The tension in the initial state, F, is determined from a static equilibrium solution. This allows the relationship,

$$F = EA\,\gamma_o\Big|_{\substack{\text{initial}\\ \text{state}}} = EA\left(\frac{\frac{dr}{ds} - \frac{ds_o}{ds}}{\frac{ds_o}{ds}}\right),$$

which can be used to express

$$\frac{ds_o}{ds} = \frac{dr}{ds}\Big/\left(\frac{F}{EA} + 1\right)$$

From this, the strain-displacement relationship becomes

$$\gamma_o = \frac{\left[\left(\frac{\partial x}{\partial s} + \frac{\partial v}{\partial s}\right)^2 + \left(\frac{\partial y}{\partial s} + \frac{\partial w}{\partial s}\right)^2\right]^{1/2}\left(\frac{F}{EA} + 1\right)}{\left[\left(\frac{\partial x}{\partial s}\right)^2 + \left(\frac{\partial y}{\partial s}\right)^2\right]^{1/2}} - 1 .$$

3.4 Equation of Motion

In the equation of motion, we shall consider the body forces of $\omega_o(s)$, cable weight per foot directed vertically, and $\vec{p}(s)$, any externally applied force per foot of arc length. This force need only be piecewise continuous and will represent the concentrated loads to be considered. Tensions at the cable element cross sections are directed along the cable's tangent. The force balance on this element (fig. 5) can be written down immediately as

$$\frac{\partial (T\vec{t})}{\partial s} + \vec{p} + \omega_o \vec{j} = \frac{\omega_o}{g} \frac{\partial^2 \vec{u}}{\partial t^2} \;..$$

For our solution, this is most conveniently expressed in its horizontal and vertical components as follows for x-direction

$$\frac{\partial}{\partial s}\left[T \frac{\frac{\partial x}{\partial s} + \frac{\partial v}{\partial s}}{\sqrt{\left(\frac{\partial x}{\partial s} + \frac{\partial v}{\partial s}\right)^2 + \left(\frac{\partial y}{\partial s} + \frac{\partial w}{\partial s}\right)^2}}\right] + p_x = \frac{\omega_o}{g} \frac{\partial^2 v}{\partial t^2}$$

and y-direction

$$\frac{\partial}{\partial s}\left[T \frac{\frac{\partial y}{\partial s} + \frac{\partial w}{\partial s}}{\sqrt{\left(\frac{\partial y}{\partial s} + \frac{\partial v}{\partial s}\right)^2 + \left(\frac{\partial y}{\partial s} + \frac{\partial w}{\partial s}\right)^2}}\right] + p_y + \omega_o = \frac{\omega_o}{g} \frac{\partial^2 w}{\partial t^2} \;.$$

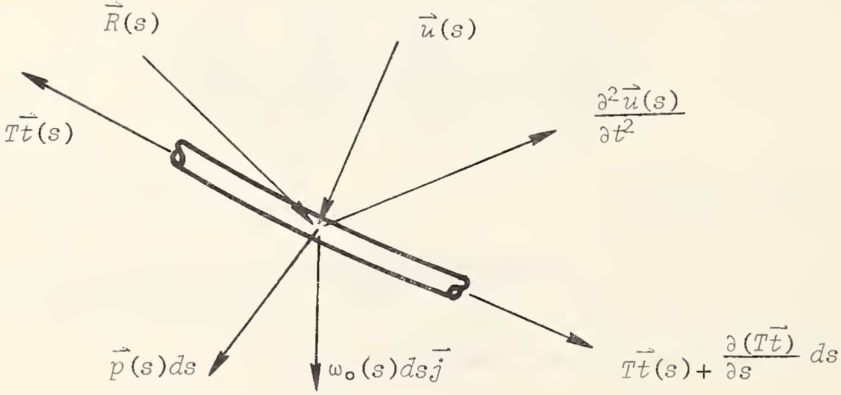
$\vec{R}(s)$
$\vec{u}(s)$
$\frac{\partial^2 \vec{u}(s)}{\partial t^2}$
$T\vec{t}(s)$
$\vec{p}(s)ds$
$\omega_o(s)ds\vec{j}$
$T\vec{t}(s) + \frac{\partial (T\vec{t})}{\partial s} ds$

Figure 5.—Forces on cable element.

3.5 Finite-Difference Solution

To conduct a preliminary investigation of the cable problem, an explicit, finite difference scheme was prepared. Some reference to the modeling of shell dynamics was made in preparing this algorithm.

The node network consists of a series of alternating stress and mass points. The mass is considered concentrated at the mass points, and the tension acts at the stress points. The appropriate parameters are evaluated at each point (fig. 6).

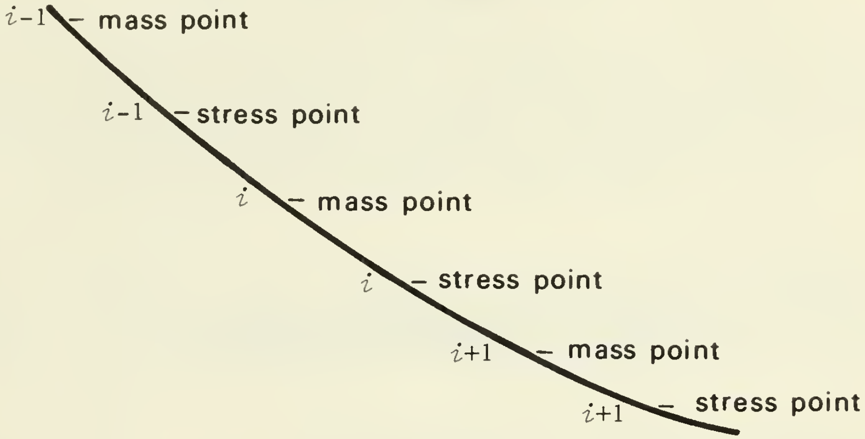

Figure 6.—Node arrangement for finite-difference solution.

Mass points.--The displacements are evaluated at the mass points. Body forces, ω_o and p, masses, and accelerations are also determined at these points.

The finite difference expressions are as follows for accelerations

$$\ddot{v}_i = \frac{\left[\left(p_x\right)_i + \dfrac{T_i \left[\dfrac{\dfrac{\partial x}{\partial s} + \dfrac{\partial v}{\partial s}}{q} \right]_i - T_{i-1} \left[\dfrac{\dfrac{\partial x}{\partial s} + \dfrac{\partial v}{\partial s}}{q} \right]_{i-1}}{\partial s} \right]}{(\omega_o)_i / g}$$

and

$$\ddot{w}_i = \frac{(\omega_o)_i + \left(p_y\right)_i + \dfrac{T_i \left[\dfrac{\dfrac{\partial y}{\partial s} + \dfrac{\partial w}{\partial s}}{q} \right]_i - T_{i-1} \left[\dfrac{\dfrac{\partial y}{\partial s} + \dfrac{\partial w}{\partial s}}{q} \right]_{i-1}}{\partial s}}{(\omega_o)_i / g} ,$$

where

$$q_i = \left[\left(\frac{\partial x}{\partial s} + \frac{\partial v}{\partial s}\right)^2 + \left(\frac{\partial y}{\partial s} + \frac{\partial w}{\partial s}\right)^2\right]^{1/2}$$

and where T and the gradients are stress point variables.

The displacements are evaluated from the accelerations with the central difference expression

$$\ddot{d}(t + \Delta t) = \frac{d(t + \Delta t) - 2d(t) + d(t - \Delta t)}{\Delta t^2}$$

or

$$\ddot{d}(t + \Delta t) = \frac{[d(t + \Delta t) - d(t)] - [d(t) - d(t - \Delta t)]}{\Delta t^2} ,$$

which can be expressed as

$$\ddot{d}(t + \Delta t) = \frac{\Delta d(t + \Delta t) - \Delta d(t)}{\Delta t^2} .$$

This gives the following expressions for displacements:

$$v_i(t + \Delta t) = v_i(t) + [\ddot{v}_i(t)\ \Delta t^2 + \Delta v_i(t)]$$

and

$$w_i(t + \Delta t) = w_i(t) + [\ddot{w}_i(t)\ \Delta t^2 + \Delta w_i(t)] .$$

Stress points.--The displacement gradients, tangent vectors, and element strains are computed at the stress points. The tensions influencing the adjacent mass points are also evaluated here.

The stress point variables are completely evaluated from adjacent mass point information. The gradients come directly from the displacements as

$$\left(\frac{\partial x}{\partial s}\right)_i = \frac{x_{i+1} - x_i}{ds} .$$

.
.
.

The strain and tension also follow directly from the mass point information as

$$\left(\gamma_{o}\right)_{i} = \frac{\sqrt{\left(x_{i+1} - x_{i} + v_{i+1} - v_{i}\right)^{2} + \left(y_{i+1} - y_{i} + w_{i+1} - w_{i}\right)^{2}}}{\sqrt{\left(x_{i+1} - x_{i}\right)^{2} + \left(y_{i+1} - y_{i}\right)^{2}} \Big/ \left(\frac{F_{i}}{EA} + 1\right)} - 1$$

and

$$T_{i} = EA\left(\gamma_{\sigma}\right)_{i} \ .$$

The central difference equations used here assume that the stress points are midway between mass points and mass points are midway between stress points, along the cable arc length. This is not strictly true; however, the variations observed are negligible and can be ignored.

4.0 PRELIMINARY RESULTS

The finite difference solution is applied to two examples to investigate potential problem areas. Two major problems encountered in this preliminary study were limiting compression in the cable and accounting for energy variations during the cable vibrations.

4.1 Examples Studied

The response to the sudden application of a midspan mass is examined. The static configuration described in figure 7 is the initial state of the two examples studied. This represents a completely flexible cable, pinned at its anchor points and hanging under the load of its own weight, assumed to be uniformly distributed along its length. The catenary expressions are used as the governing equation.

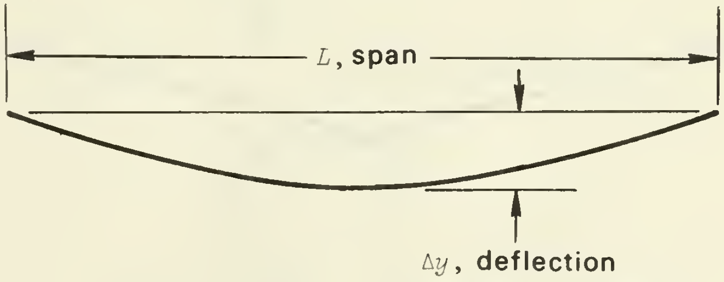

L, span = 1,003.53 feet
Δy, deflection = 100.72 feet
s, line length = 1,030.0 feet
ω, line weight per foot = 3.16 pounds/foot
E, cable modulus = 1.9×10^{7} pounds/square inch
A, reference cross section = 0.85 square inch
H, tension at midspan = 4,001.5 pounds

Figure 7.—Initial state of cable in example problems.

The final static state of the two examples is established to serve as reference points in the energy studies. The two configurations, 2,000-pound loading and 5,000-pound loading (both at midspan), as described in figures 8 and 9, represent gradual application of the loads. The final state line lengths are compatible with the linear stress-strain relationship used. The reference displacement, Δy_{ref}, is defined as the deflection the load experiences when gradually applied. The values are given in the figures.

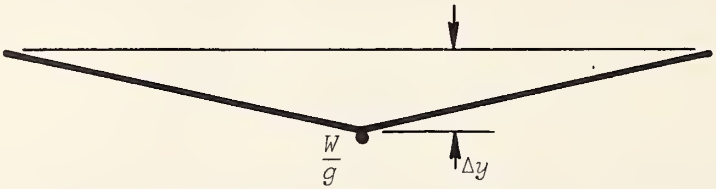

W, weight of load = 2,000.0 pounds

T, tension at anchors = 8,446.98 pounds

Δy, static deflection = 113.01 feet

Δy_{ref}, deflection from initial state = 12.29 feet

s, line length = 1,030.262 feet

Figure 8.—Final static state of 2,000.0-pound load.

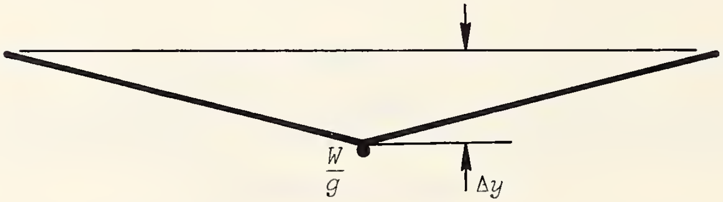

W, weight of load = 5,000.0 pounds

T, tension at anchors = 14,860.45 pounds

Δy, static deflection = 116.372 feet

Δy_{ref}, deflection from initial state = 15.652 feet

s, line length = 1,030.67 feet

Figure 9.—Final static state of 5,000.0-pound load.

4.2 Energy Considerations

During the investigation of response, the strain, kinetic, and potential energies were monitored. The energies were defined and organized to distinguish between:

4.2.1 Strain energy in the cable,
4.2.2 Kinetic energy in the cable,
4.2.3 Kinetic energy in the load,
4.2.4 Potential energy of the cable, and
4.2.5 Potential energy of the load.

These were all normalized with the total energy of the system as computed from initial conditions.

4.2.1 Strain energy in the cable

The strain energy during motion is computed as a summation over all elements, namely,

$$SE = \sum_{i}^{N} 1/2\ T\gamma_o \Delta s_o \ .$$

The initial strain energy is computed from the catenary expressions as

$$SE_I = 2m \int_{\left(\frac{x}{m}\right)_{LOAD}}^{\frac{L}{2m}} 1/2\ T\gamma_o \frac{ds}{dx}\ d\left(\frac{x}{m}\right)$$

and with

$$T = \omega_o m \cosh \frac{x}{m} \ ,$$

$$\gamma_o = \frac{ds}{ds_o} - 1 = \frac{T}{EA} \ ,$$

$$s = m\left(\sinh \frac{x}{m} - \sinh\left(\frac{x}{m}\right)_{LOAD}\right) , \quad \text{and}$$

$$\frac{ds}{dx} = \cosh \frac{x}{m} \ .$$

Where m is the catenary parameter equal to horizontal tension over line weight per foot, this becomes

$$SE_I = m \int_{\left(\frac{x}{m}\right)_{LOAD}}^{\frac{L}{2m}} \frac{(\omega_o m)^2 \cosh^3 \frac{x}{m}}{EA} \, d\left(\frac{x}{m}\right)$$

or

$$SE_I = \frac{m}{4} \frac{(\omega_o m)^2}{EA} \left(1/3 \sinh \left(3\frac{x}{m}\right) + 3 \sinh \left(\frac{x}{m}\right)\right) \Bigg|_{\left(\frac{x}{m}\right)_{LOAD}}^{\frac{L}{2m}}$$

4.2.2 Kinetic energy in the cable

This energy is computed as

$$(KE)_{CABLE} = \sum_i^N 1/2 \left(\frac{\omega_o}{g}\right) \Delta s \; (\dot{v}_i^2 + \dot{w}_i^2) \; .$$

The initial conditions of the examples have no kinetic energy.

4.2.3 Kinetic energy in the load

This is simply computed as

$$(KE)_{LOAD} = 1/2 \; \frac{LOAD}{g} \; (\dot{v}^2_{LOAD} + \dot{w}^2_{LOAD}) \; .$$

4.2.4 Potential energy of the cable

The cable's potential energy is also monitored during motion. The datum plane assumed is horizontal and intersects the load point resulting when loads are gradually applied. The finite difference scheme monitors the summation over all segments

$$(PE)_{CABLE} = \sum_i^N (\omega_o \Delta s)(\Delta y_{ref} + y_{LOAD} - y_i - w_i) \; .$$

The initial potential energy is evaluated from the catenary expressions as

$$\left(PE_I\right)_{CABLE} = 2\omega_o m \int_{\left(\frac{x}{m}\right)_{LOAD}}^{\frac{L}{2m}} (\Delta y_{ref} + m \cosh \frac{x}{m} - m) \frac{ds}{dx} \, d(\frac{x}{m}) \; .$$

Upon integration, this becomes

$$\left(PE_I\right)_{CABLE} = 2(\omega_o m)\left[(\Delta y_{ref} - m)\sinh \frac{x}{m} + m\left(\frac{\sinh \frac{2x}{m}}{4} + \frac{x}{2m}\right)\right]\Bigg|_{\left(\frac{x}{m}\right)_{LOAD}}^{\frac{L}{2m}}$$

4.2.5 Potential energy of the load

The potential energy of the load is simply

$$(PE)_{LOAD} = (LOAD)(\Delta y_{ref} - \omega_{LOAD})$$

during motion and

$$\left(PE_I\right)_{LOAD} = (LOAD)(\Delta y_{ref})$$

initially.

The total initial energy for each example is

$$TE_I = SE_I + \left(PE_I\right)_{CABLE} + \left(PE_I\right)_{LOAD} \; .$$

This is used to normalize the other energies resulting in definition of the following ratios,

$$se = \frac{SE}{TE_I} \; ,$$

$$pe = \frac{(PE)_{CABLE} + (PE)_{LOAD}}{TE_I} \; , \text{ and}$$

$$ke = \frac{(KE)_{CABLE} + (KE)_{LOAD}}{TE}$$

These ratios are plotted and discussed.

4.3 Finite Difference Routine

The finite difference routine described previously was implemented in FORTRAN IV on the University of Washington's CDC 6400. The initial segment length to be used in the examples was established during program development. A segment length of 51.5 feet seemed to provide the necessary accuracy. The time increment was established from the relationship

$$\Delta t \leq \Delta s \sqrt{\frac{\rho}{E}} \ .$$

A time step of .01/3 second was used except where indicated in the study of energy.

5.0 DISCUSSION OF RESULTS

The behavior of tensions over a 10-second period is plotted for both examples in figure 10. The vertical deflection of the load point and the horizontal deflection of a point midway between the load and the right anchor are plotted in figures 11 and 12, respectively.

Figure 10 demonstrates the need for this study. Accepted design procedures would have sized the cable for the 5,000-pound case to withstand 44,580 pounds of tension (three times the tension in the final static state). Under these conditions, this cable would have broken.

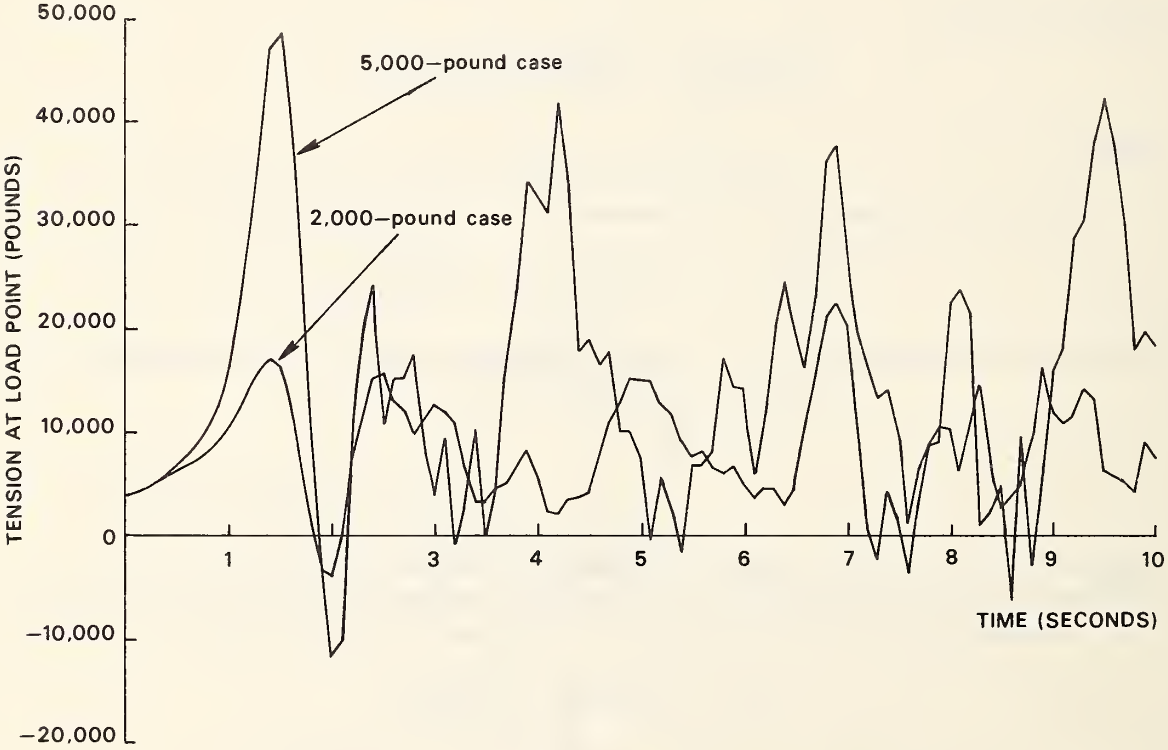

Figure 10.—Comparison of load point tensions.

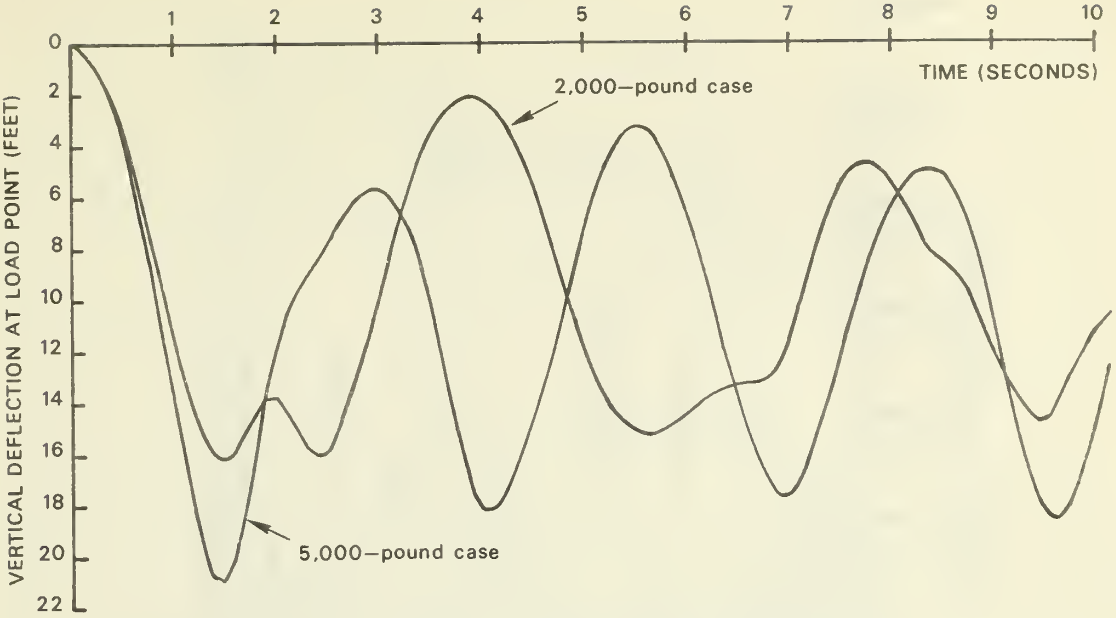

Figure 11.–Comparison of load point vertical deflections.

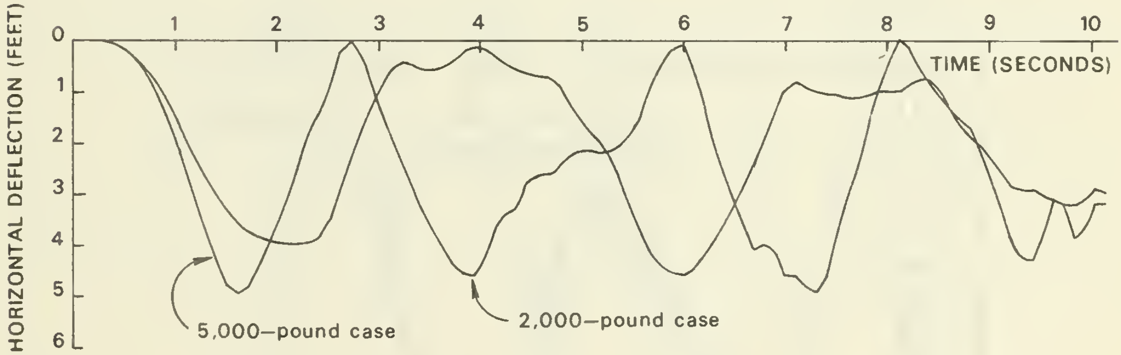

Figure 12.–Comparison of horizontal deflections (monitored midway between the load and the right anchor).

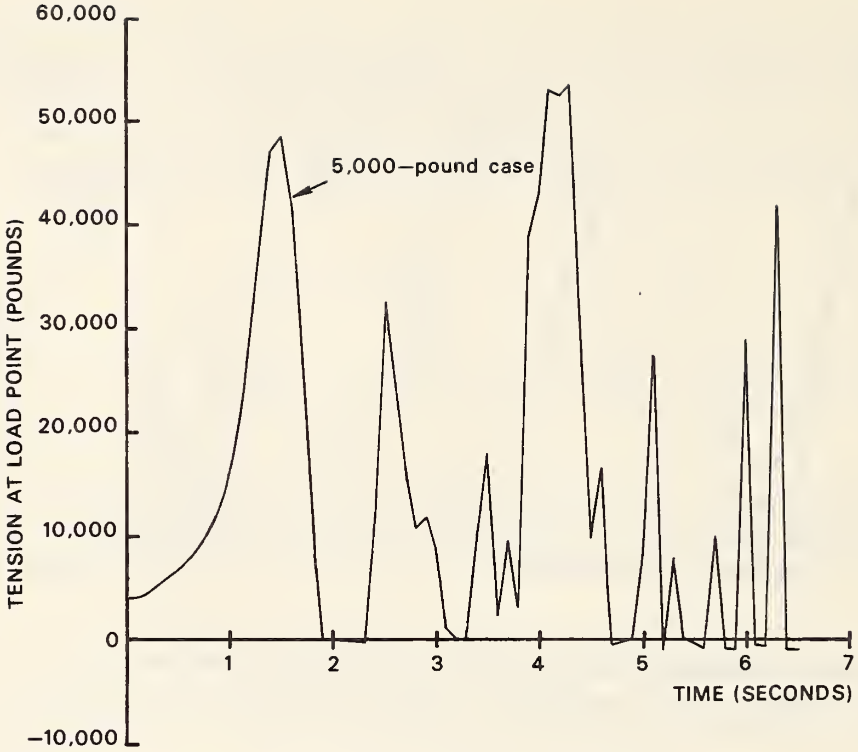

Figure 13.—Tension in compression-limited case.

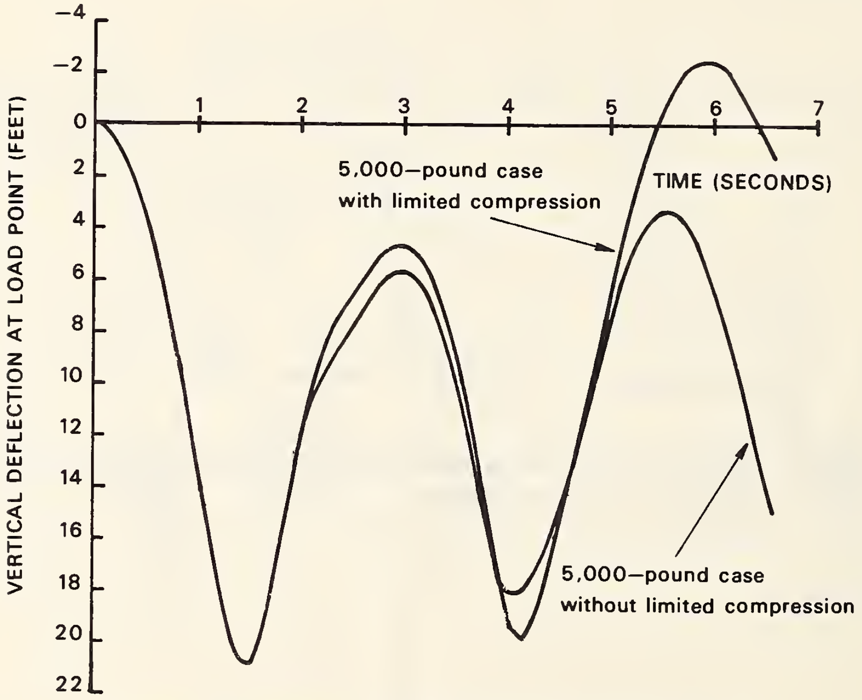

Figure 14.—Comparison of load point vertical deflections.

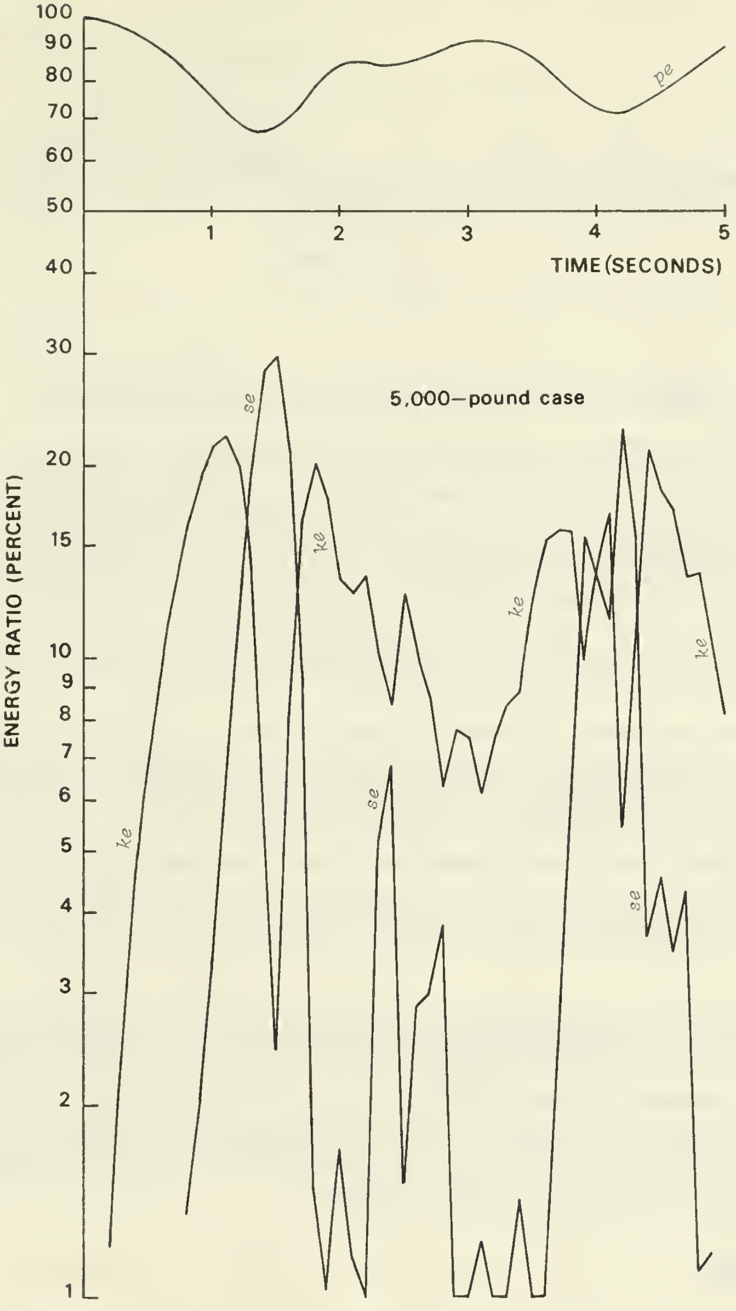

Figure 15.—Comparison of energy ratios.

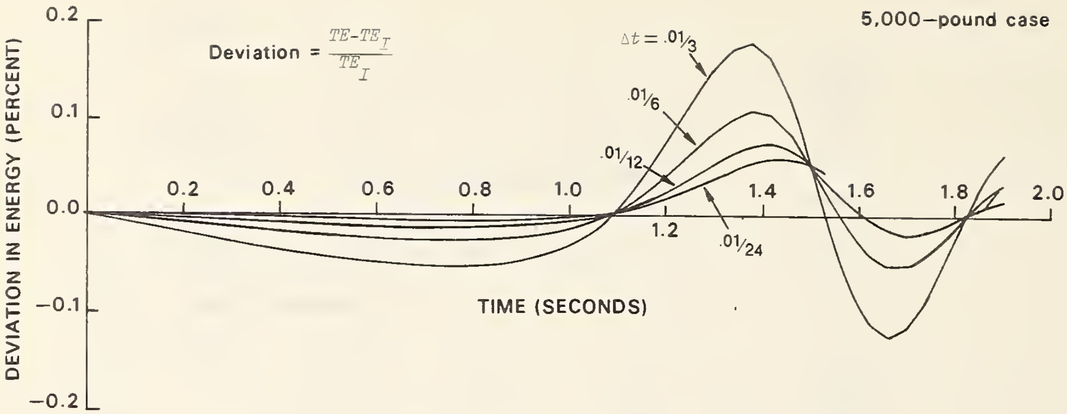

Figure 16.—Energy deviations with different time increments.

Although the relatively uniform behavior of the deflection curves suggests that an analytic prediction might be possible, the deflection response is deceptive as an indicator of tensions. This is apparent since the erratic behavior of the tension is not clearly indicated by the deflections. The deflections, however, may serve to predict the upper bound on tensions. For example, the 20.8-foot deflection in the 5,000-pound case would imply a 21,100-pound load, causing 48,300 pounds of tension. The peaks occurring later do not reach this level of tension since at these points more energy is in kinetic form.

The tensions displayed in figure 10 were allowed to experience negative values (compression) to maintain stability in the computations. Figure 13 shows the 5,000-pound case, limited to a physically more realistic maximum of 1,000 pounds compression, which generated instabilities that were out of control by 6.5 seconds. Again, the response of vertical deflection, compared in figure 14 to the 5,000-pound case allowing compression was deceptive. This situation is presently the major problem in the analysis. Bending resistance, introduced in an attempt to solve this problem, also failed to control the situation.

Strain, kinetic, and potential energy distributions are displayed in figure 15. The uniform behavior of the potential energy could be expected since the vertical deflection response is also uniform. The erratic behavior of the strain and kinetic energies are comparable to the tension response. These fluctuations are probably the major cause of the variations in the total energy plotted in figure 16. It is clear that smaller time increments reduce the fluctuations in total energy.

6.0 CONCLUSION

A study of previous work done in the area of cable dynamics has revealed very little that is applicable to the skyline logging problem. The configurations and loading conditions experienced by the logging skyline distinguish it as a unique problem in cable dynamics. The preliminary results presented in this note clearly point out the need for further study. This work should continue on an analytical basis until a reliable simulation model can be formed. Eventually an experimental program to aid in model development and checkout should be conducted.

LITERATURE CITED

1. American Society of Civil Engineers.
1943. The failure of the Tacoma Narrows bridge. Amer. Soc. Civil Eng. Proc.

2. Anderson, Samuel Herbert.
1921. Tensions in track cables and logging skylines. Univ. Wash. Eng. Exp. Sta. Bull. 13, 27 p., illus.

3. Carrier, G. F.
1945. On the non-linear vibration problem of the elastic string. Quart. Appl. Math. 3: 157-165.

4. ______
1949. A note on the vibrating string. Quart. Appl. Math. 7: 97-101.

5. Carson, Ward W., and Charles N. Mann.
1970. A technique for the solution of skyline catenary equations. Pac. Northwest Forest & Range Exp. Sta. USDA Forest Serv. Res. Pap. 110, 18 p., illus.

6. Cole, J. D., C. B. Dougherty, and H. J. Huth.
1953. Constant strain waves in strings. J. Appl. Mech. 20: 519.

7. Coulson, Charles Alfred.
1949. Waves, a mathematical account of the common types of wave motion. 5th ed., 159 p., illus. New York: Interscience.

8. Inglis, Charles Edward.
1963. Applied mechanics for engineers. Ch. IV. New York: Dover Publ.

9. Jawerth, D., and H. Schulz.
1966. Ein beitrah zur frage der eigen schwingungen, windanfachenden krafte und aerodynamischen stabilitat bei hangenden dachern. Der Stahlbau 35(1): 1-8.

10. Mills, R.
1932. Tensions in logging skylines. Univ. Wash. Eng. Exp. Sta. Bull. 66, 30 p., illus.

11. Moisil, G. C.
1956. Shock waves in cables. 9th Int. Congr. Appl. Mech. Proc.

12. Mollmann, H.
1965. A study in the theory of suspension structures. 229 p., illus. Akad. Forlag.

13. O'Brien, T., and A. J. Francis.
1964. Cable movements under two-dimensional loads. J. Struct. Div., Amer. Soc. Civil Eng. Proc., p. 89.

14. Otto, Frei.
1954. The suspended roof. Berlin: Ullstein A. G.

15. Pugsley, A. G.
1949. On the natural frequencies of suspension chains. Quart. J. Mech. Appl. Math. 2(4): 412-418.

16. ______
1949. Some experimental work on model suspension bridges. J. Struct. Eng. 27: 327-348.

17. Reissner, H.
1943. Oscillations of suspension bridges. J. Amer. Soc. Mech. Eng. Trans. 65: A23-A32.

18. Ringleb, F. O.
1957. Motion and stress of an elastic cable due to impact. J. Appl. Mech. 24: 417.

19. Scalzi, J. B., W. Podolny, and W. C. Teng.
1969. Design fundamentals of cable roof structures. U.S. Steel Corp. ADUSS 55-3580-01, 140 p.

20. Schneider, L., T. Mahan, and L. G. Burton.
1964. Tow cable snap loads. Winter Annu. Meet., Amer. Soc. Mech. Eng. 64-WA/UNT-8, 8 p., illus.

21. Steinman, D. B.
1943. Rigidity and aerodynamic stability of suspension bridges. Amer. Soc. Civil Eng. Proc. 69(9): 1361-1397.

22. Tsubol, Y., and M. Kawaguchi.
1964. Suspension structure for the Tokyo Olympics. High-Rise & Long-Span Struct., Japan Soc. Promot. Sci., Symp. Proc.

23. ______ and M. Kawaguchi.
1966. Probleme beim ent wurf einer hangedachkonstruktion anhand des beispiels der schwunmhalle fur die Olympischen Spiele 1964 in Tokio. Der Stahlbau 35: 65.

24. Vadman, David Russell.
1968. Suspension roof structures. Master's thesis. Univ. Wash. TA/7/Th16707.

The mission of the PACIFIC NORTHWEST FOREST AND RANGE EXPERIMENT STATION is to provide the knowledge, technology, and alternatives for present and future protection, management, and use of forest, range, and related environments.

Within this overall mission, the Station conducts and stimulates research to facilitate and to accelerate progress toward the following goals:

1. Providing safe and efficient technology for inventory, protection, and use of resources.
2. Development and evaluation of alternative methods and levels of resource management.
3. Achievement of optimum sustained resource productivity consistent with maintaining a high quality forest environment.

The area of research encompasses Oregon, Washington, Alaska, and, in some cases, California, Hawaii, the Western States, and the Nation. Results of the research will be made available promptly. Project headquarters are at:

College, Alaska
Juneau, Alaska
Bend, Oregon
Corvallis, Oregon
La Grande, Oregon
Portland, Oregon
Roseburg, Oregon
Olympia, Washington
Seattle, Washington
Wenatchee, Washington

The FOREST SERVICE of the U.S. Department of Agriculture is dedicated to the principle of multiple use management of the Nation's forest resources for sustained yields of wood, water, forage, wildlife, and recreation. Through forestry research, cooperation with the States and private forest owners, and management of the National Forests and National Grasslands, it strives — as directed by Congress — to provide increasingly greater service to a growing Nation.